

An overview of the photon beam properties from the European XFEL operating with new baseline parameters of the electron beam: status of April 2010

E.A. Schneidmiller, M.V. Yurkov

Deutsches Elektronen-Synchrotron (DESY), Hamburg, Germany

Abstract

A new set of baseline parameters of the electron beam is under discussion in the framework of the European XFEL project [1–3]. This note presents an overview of the radiation properties generated by SASE FEL radiators driven by electron beam with revised baseline parameters of the electron beam [3]. Parameter space of the electron beam covers bunch charges from 0.1 nC to 1 nC, and operating energies 17.5 GeV and 14 GeV.

Contents

1	Introduction	2
2	Definition of the radiation characteristics	3
3	Tunability range	5
4	General properties of the radiation from SASE1 and SASE2	8
5	An overview of saturation properties of SASE1	22
6	Operation of SASE3 as an afterburner	27
7	Design formulae for an optimized XFEL	29
	References	33

1 Introduction

Recent success of the Linac Coherent Light Source (LCLS) demonstrated feasibility for reliable production, compression, and acceleration of electron beams with small emittance. Currently LCLS provides different modes of operation with different charges (20 pC to 250 pC), different peak currents (1.x kA to 3.x kA) and wide wavelength range (0.12 nm to 2.2 nm) [4]. Conceptual Design Report of LCLS considered two possible options of the LCLS operation: baseline with bunch charge of 1 nC and low charge option with bunch charge of 250 pC [5]. An option with 1 nC bunch charge was based on rather conservative value of the normalized emittance of 1.2 mm-mrad assuming some set of possible physical effects and technical imperfections leading to emittance degradation. Optimistic analysis of the low charge option predicted much smaller value of the emittance of about 0.4 mm-mrad. In practice small charge option has been realized experimentally.

Similar level of concerns of possible problems of physical and of technical nature has been accepted in the European XFEL project as well: baseline option assumed operation with the bunch charge of 1 nC and value of the normalized emittance 1.4 mm-mrad [6]. However, recent trends and experimental results provided the base for revision of the baseline parameters. First we refer to successful operation of FLASH free electron laser which serves as a prototype of the European XFEL. In particular, thorough analysis of the radiation properties generated by FLASH gave an indication on a small value of the slice emittance of about 1 mm-mrad [7]. Recent results of the Photo Injector Test Facility in Zeuthen (PITZ) demonstrated the possibility to generate electron beams with smaller charge and emittance [8, 9]. Computer modelling of the beam formation system at the European XFEL also indicate on the possibility to preserve electron beam quality during

Table 1

Properties of the electron beam at the undulator entrance
(New baseline parameters, April 2010 [3])

Bunch charge	nC	0.1	0.25	0.5	1
Peak beam current	A	2500	3000	4000	5000
Normalized rms emittance	mm-mrad	0.42	0.6	0.77	1.05
rms energy spread	MeV	3	2.6	2.3	2
rms pulse duration	fs	12	25	40	60

Table 2

Properties of the electron beam at the undulator entrance
(Baseline parameters, TDR 2006 [6])

Bunch charge	nC	1
Peak beam current	A	5000
Normalized rms emittance	mm-mrad	1.4
rms energy spread	MeV	1
rms pulse duration	fs	80

acceleration and compression [1, 2]. Recently all these trends have been analyzed, and a new baseline parameter set for the electron beam parameters has been fixed (see Table 1) [3]. Parameter space has been significantly extended in terms of the bunch charge. As a result, different modes of FEL operation become possible with essentially different properties of the radiation. In this paper we present an overview of radiation properties of SASE FEL radiators driven by electron beam with new baseline parameters. In view of current discussion on potential change of the nominal energy of the accelerator from 17.5 GeV to 14 GeV we illustrate both options where data are available. An overview of such a wide parameter space was impossible without application of fitting formulae based on application of similarity techniques to the results of extended numerical simulations [10–12]. To make an overview to be consistent we present here basic set of fitting formulae describing operation of an optimized SASE FEL. In the general case FEL process is simulated with time-dependent FEL simulation code FAST [13].

2 Definition of the radiation characteristics

Due to start-up of the amplification from the shot noise in the electron beam Self-Amplified Spontaneous Emission Free Electron Laser (SASE FEL) produces random fields \tilde{E} in time and space. Integration of the power density $I = |\tilde{E}|^2$ over transverse cross section of the photon beam gives us instantaneous radiation power, $P \propto \int I \, d\vec{r}_\perp$. Averaging of the radiation power along the pulse gives us averaged radiation power, and integration of the radiation power along the pulse gives the radiation pulse energy. Partial longitudinal coherence is formed due to slippage effect, and partial transverse coherence is formed due to diffraction effects. We describe radiation fields generated by a SASE FEL in terms of statistical optics [14, 15]. Longitudinal and transverse coherence are described in terms of correlation functions. The first order time correlation function, $g_1(t, t')$, is defined as:

$$g_1(\vec{r}, t - t') = \frac{\langle \tilde{E}(\vec{r}, t) \tilde{E}^*(\vec{r}, t') \rangle}{\left[\langle |\tilde{E}(\vec{r}, t)|^2 \rangle \langle |\tilde{E}(\vec{r}, t')|^2 \rangle \right]^{1/2}}. \quad (1)$$

For a stationary random process the time correlation functions are dependent on only one variable, $\tau = t - t'$. The coherence time is defined as [15]:

$$\tau_c = \int_{-\infty}^{\infty} |g_1(\tau)|^2 \, d\tau. \quad (2)$$

The transverse coherence properties of the radiation are described in terms of the transverse correlation functions. The first-order transverse correlation function

is defined as

$$\gamma_1(\vec{r}_\perp, \vec{r}'_\perp, z, t) = \frac{\langle \tilde{E}(\vec{r}_\perp, z, t) \tilde{E}^*(\vec{r}'_\perp, z, t) \rangle}{\left[\langle |\tilde{E}(\vec{r}_\perp, z, t)|^2 \rangle \langle |\tilde{E}(\vec{r}'_\perp, z, t)|^2 \rangle \right]^{1/2}} .$$

We consider the model of a stationary random process, meaning that γ_1 does not depend on time. We define the degree of transverse coherence as [10]:

$$\zeta = \frac{\int |\gamma_1(\vec{r}_\perp, \vec{r}'_\perp)|^2 I(\vec{r}_\perp) I(\vec{r}'_\perp) d\vec{r}_\perp d\vec{r}'_\perp}{\left[\int I(\vec{r}_\perp) d\vec{r}_\perp \right]^2} . \quad (3)$$

Physical sense of this definition for ζ is the inverse number of transverse modes in the radiation pulse (see ref. [10] for more details).

The degeneracy parameter δ is defined as the number of photons per mode (coherent state):

$$\delta = \dot{N}_{ph} \tau_c \zeta , \quad (4)$$

where \dot{N}_{ph} is the photon flux. Peak brilliance of the radiation from an undulator is defined as a transversely coherent spectral flux:

$$B_r = \frac{\omega d \dot{N}_{ph}}{d\omega} \frac{\zeta}{(\lambda/2)^2} = \frac{4\sqrt{2}c\delta}{\lambda^3} . \quad (5)$$

When deriving right-hand term of the equation we used the fact that the spectrum shape of SASE FEL radiation in a high-gain linear regime and near saturation is close to Gaussian [15]. In this case the rms spectrum bandwidth σ_ω and coherence time obey the equation $\tau_c = \sqrt{\pi}/\sigma_\omega$.

Figure 1 shows evolution of main characteristics of SASE FEL along the undulator: brilliance, radiation power, degree of transverse coherence, and coherence time (this is numerical example typical for an x-ray FEL). For a considered parameter range the radiation power grows continuously along the undulator, so that there is no position where it achieves the maximum (what is usually understood as saturation point). On the other hand, if one traces evolution of the brilliance (or, degeneracy parameter) of the radiation along the undulator length there is always the point, which we define as the saturation point, where the brilliance reaches maximum value [10–12]. This always happens because transverse and longitudinal coherence get worse in the nonlinear regime and lead to a decrease of the brilliance despite the fact that the power grows steadily. We can formulate qualitatively that in the nonlinear regime coherence properties degrade faster than increase of the radiation power.

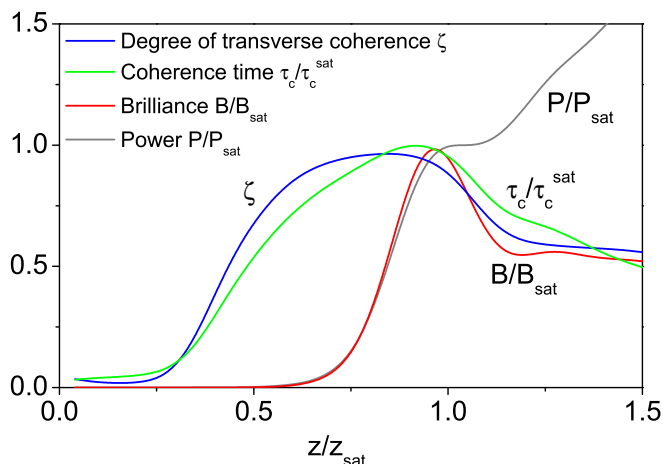


Fig. 1. Evolution of main characteristics of SASE FEL along the undulator: brilliance (red line), radiation power (black line), degree of transverse coherence (blue line), and coherence time (green line). Brilliance and radiation power are normalized to saturation values. Coherence time is normalized to the maximum value. Undulator length is normalized to saturation length. The plot has been derived from the parameter set corresponding to $2\pi\epsilon/\lambda = 1$. Calculations have been performed with the simulation code FAST [13].

In the following we present characteristics of the radiation at the saturation point defined as the point where brilliance of the radiation reaches maximum value. We should state that in the Technical Design Report 2006 [6] and early studies we used a qualitative definition of the saturation point. As a consequence, saturation power may be uncertain within a factor of two. It has been also assumed that the radiation from a SASE FEL has nearly complete transverse coherence. The use of the strict definition and accounting for a finite degree of transverse coherence leads to the reduction of saturation parameters presented in earlier studies (and in the TDR 2006 [6] as well) by a factor of 2-3.

3 Tunability range

Technical Design Report of the European XFEL assumes nominal energy of the electron beam of 17.5 GeV and installation of three undulators covering wavelength range from 0.1 to 1.6 nm [6]. SASE1 is optimized for operation around 0.1 nm, SASE2 covers wavelength range 0.1 nm - 0.4 nm, and SASE3 operates in the wavelength range 0.4 nm - 1.6 nm. Longer wavelength are achieved by means of operation of the driving accelerator at the reduced energy of 10 GeV. Undulators are designed with planar NdFeB technology which imply interdependence of the

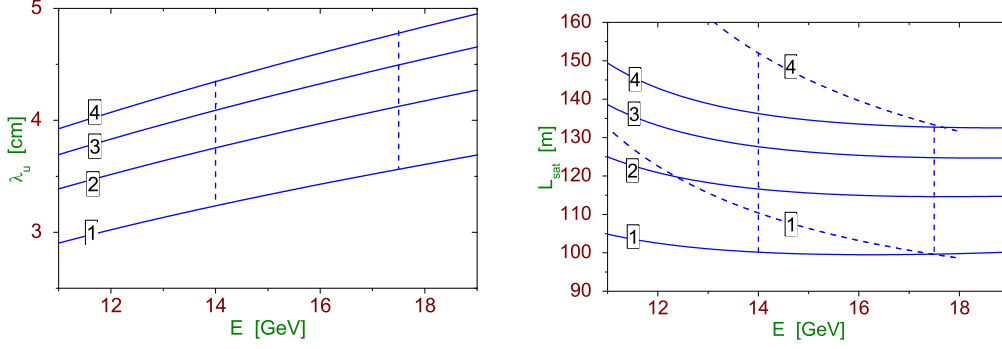


Fig. 2. Undulator period (left plot) versus electron beam energy for different values of maximum radiation wavelength of 0.1 nm, 0.2 nm, 0.3 nm, and 0.4 nm. Minimum undulator gap is equal to 10 mm. Plot on the right-hand side shows corresponding saturation length for SASE FEL tuned to 0.1 nm wavelength. Parameters of the electron bunch correspond to 1 nC option from Table 1. Dashed curves show operation of SASE FEL with non-optimized undulator (see the text).

peak magnetic field B_{\max} and ratio of the gap to the undulator period g/λ_w [6]:

$$B_{\max}[\text{T}] = 3.694 \exp \left[-5.068 \frac{g}{\lambda_w} + 1.52 \left(\frac{g}{\lambda_w} \right)^2 \right]. \quad (6)$$

This fit is valid for $0.1 < g/\lambda_w < 1$. The value of the undulator period is defined by the electron beam energy, minimum undulator gap, and maximum radiation wavelength. For the European XFEL minimum undulator gap is 10 mm. Universal plots for the undulator period are presented in Fig. 2. With practical accuracy provided by fitting (6) we can derive fitting formulae for the undulator period as function of electron beam energy and maximum radiation wavelength:

$$\lambda_w [\text{cm}] \simeq 0.996 \times E [\text{GeV}]^{0.445} \times \lambda_{\max} [\text{\AA}]^{0.216}. \quad (7)$$

For nominal energy of electrons of 17.5 GeV this formula gives periods of the undulator of 3.56 cm, 4.8 cm, and 6.5 cm for SASE1, SASE2, and SASE3, respectively [6]. Additional optimization of SASE3 undulator resulted in the period length of 6.8 cm [16]. Keeping the same tunability range, but calculating for nominal energy of 14 GeV results in the period lengths 3.24 cm for SASE1, 4.35 cm for SASE2, and 5.87 cm for SASE3. Plot on the right-hand side of Fig. 2 shows saturation length for SASE FEL operating at 1 Å traced for tunability range $\lambda_{\max}/\lambda_{\min} = 1$ (fixed gap), 2, 3, and 4 (solid curves 2, 3, and 4, respectively). Note that curves marked with number one refers to SASE1, and curve marked with number 4 refers to SASE2. One can see that extension of the tunability range of short-wavelength SASE FEL (SASE2 in our case) brings the penalty for the undulator length. Within parameter space of the European XFEL extension of the tunability range by a factor of four requires extra 35% of the undulator length with respect to optimized fixed

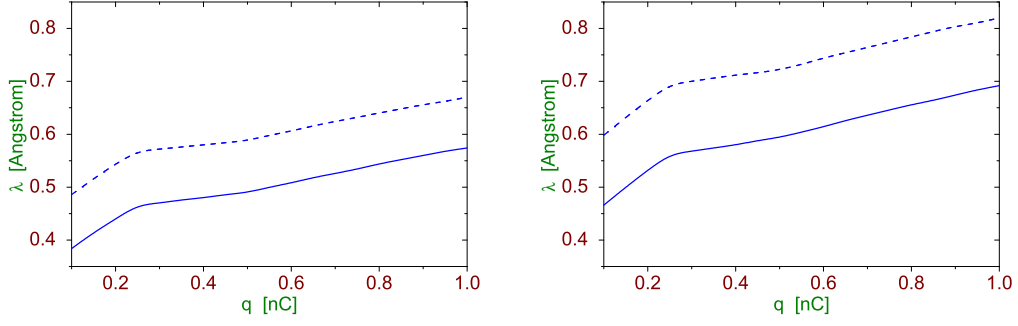


Fig. 3. Minimum wavelength of SASE1 and SASE2 (left and right plot, respectively) versus bunch charge. Undulator length is equal to 165 meters for SASE1, and 185 meters for SASE2. Solid and dashed lines correspond to electron energy of 17.5 GeV and 14 GeV, respectively.

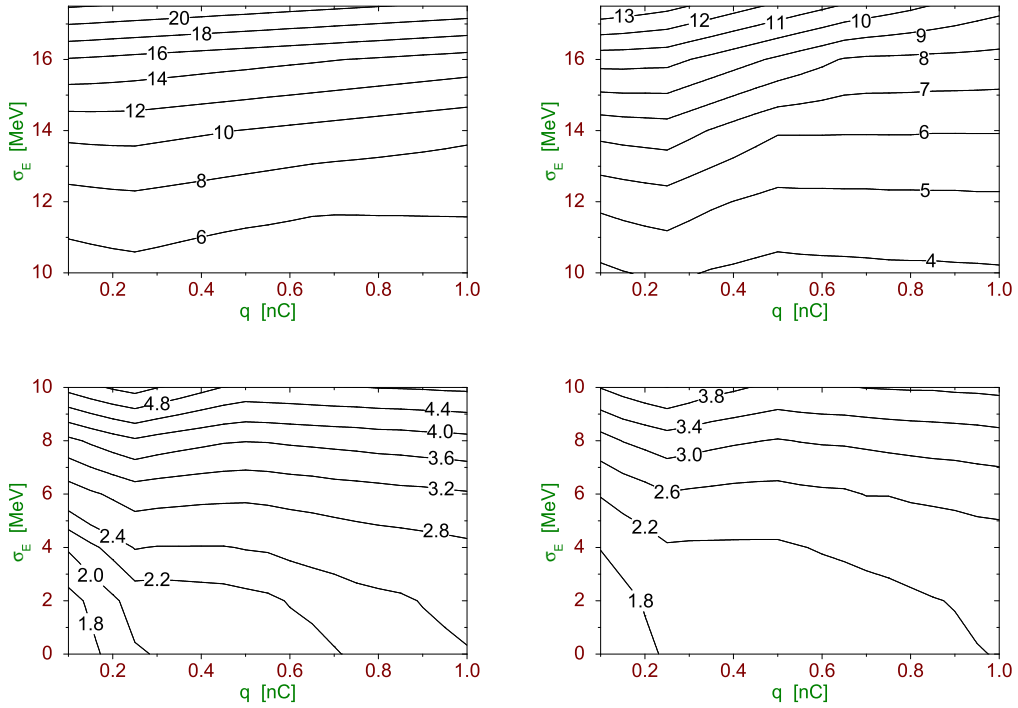


Fig. 4. Minimum wavelength (in units of \AA) of SASE3 versus bunch charge and energy spread in the electron beam. Undulator length is equal to 100 m. Focusing beta function is equal to 15 m. Plots on the left hand side and the right hand side correspond to the electron energy of 14 GeV and 17.5 GeV, respectively. Parameters of SASE3 are optimized for minimum gain length.

gap undulator (SASE1).

Another question of practical interest is operation at the reduced energy of 14 GeV of SASE1/SASE2 with undulators optimized for operation at 17.5 GeV. Dashed curves numbered with 1 and 4 in Fig. 2 show saturation length of SASE1

and SASE2 tuned to 0.1 nm at the energy of 14 GeV. We see that use of nonoptimized undulator increases saturation length by about 15% when operating at short wavelengths. On the other hand, overall tunability range becomes wider in the direction of longer wavelengths. Maximum wavelength is defined by minimum undulator gap, and it scales as $\propto 1/\gamma^2$ with electron beam energy. For SASE1 maximum wavelength is equal to 0.1 nm and 0.156 nm for electron beam energy 17.5 GeV and 14 GeV, respectively. Minimum wavelength is defined by electron beam energy, undulator length, and quality of the electron beam. We see from Fig. 3 that minimum wavelength of SASE1 and SASE2 (and hence tunability range) depends significantly on the quality of the electron beam. It differs by a factor of 1.5 for operating charge of 0.1 nC and 1 nC. Interdependence of parameters is such that minimum wavelength scales a bit slower than $\propto 1/\gamma$ in the parameter range of SASE1 and SASE2. Operation of SASE1 at 17.5 GeV allows to reach saturation at 0.05 nm with relatively large bunch charge of 0.5 nC which provides higher average photon flux and average brilliance.

Maximum wavelength of SASE3 is equal to 1.6 and 2.5 nm for electron beam energy of 17.5 GeV and 14 GeV, respectively. A concept of the European XFEL assumes to operate SASE3 as an afterburner using spent electron beam after SASE1. Influence of the energy spread in the electron beam and operating bunch charge on minimum wavelength is illustrated in Fig. 4. We note that minimum wavelength exhibits rather slow dependency on the bunch charge. Minimum wavelength for "fresh" electron bunch (energy spread around 2 MeV) is around 0.2 nm in the whole energy range from 14 GeV to 17.5 GeV. Increase of the energy spread leads to rapid increase of minimum wavelength.

4 General properties of the radiation from SASE1 and SASE2

In the following we illustrate operation of the European XFEL driven by electron beam with new baseline parameters presented in Table 1. Parameters of the undulators are those of TDR 2006 for SASE1 and SASE2 (with period length of 3.56 cm and 4.8 cm), and SASE3 is planar undulator with period length of 6.8 cm [16]. Figure 5 shows evolution of the radiation pulse energy along the undulator length of SASE1, SASE2, and SASE3 for driving energy of the electron beam of 14 GeV. One can see that the radiation pulse energy grows continuously with the undulator length. However, the value of peak brilliance reaches its maximum value in the saturation point. Table 3 presents main characteristics of the radiation for two boundaries of the operating range of charges, 0.1 nC and 1 nC and operating energy of 14 GeV. Table 4 presents extended table for SASE3. Electron bunch shape has been approximated by gaussian with rms pulse length given in Table 1. Averaged characteristics were calculated for the following pulse pattern: macropulse repetition rate 10 Hz, macropulse duration 600 μ s, and micropulse repetition rate 4.5 MHz (27000 pulses per second).

As a reference, we present also Table 5 of main SASE characteristics from the Technical Design Report 2006 [6]. Baseline parameters of the electron beam for TDR 2006 were: bunch charge 1 nC, electron beam energy 17.5 GeV, peak beam current 5 kA, rms normalized emittance 1.4 mm-mrad, rms energy spread 1 MeV, rms pulse duration 80 fs, repetition rate 30000 pulses per second (see Table 2). As we mentioned above, a qualitative definition of the saturation point has been used.

Comparison of old and new baseline parameters using tables 3 and 5 is rather complicated due to the change of many parameters simultaneously (electron beam properties, energy, repetition rate). Step-by-step comparison of TDR2006 baseline parameters and present baseline option is presented in Table 6 for SASE1 operating at the wavelength of 0.1 nm. We start with comparative analysis of SASE1 operation which involves three different scenarios: i) parameters of electron beam from TDR 2006 [6] and energy 17.5 GeV; ii) new parameters of the electron beam [3] and energy 17.5 GeV; iii) new parameters of the electron beam [3] and energy 14 GeV. Relevant results are compiled in Table 6 for SASE1 operating at the wavelength of 0.1 nm in the saturation regime. Averaged characteristics are calculated for 27000 pulses per second. The same rms length of electron bunch of 60 fs is used in all cases to simplify comparison of the radiation properties. Brilliance is calculated according to refs. [10–12] in all cases. We note that transition from TDR 2006 baseline parameters to new baseline parameters (see Tables Table 1 and 2) results in visible improvement of all characteristics of the radiation if we keep the same energy of the electron beam of 17.5 GeV. One can see that two main steps: improve of emittance (positive factor), and decrease of energy to 14 GeV (negative factor) nearly compensate each other in the range of charges around 1 nC, and bring us back in the parameter space of TDR 2006.

In this note parameters of radiation were calculated for the wavelength range defined in TDR 2006. Note, however that the improved parameters of the electron beam at small charges allow for operation at significantly shorter wavelengths, down to 0.05 nm at SASE1, although practically without contingency (see Fig. 5 and Table 3).

An important practical parameter is angular divergence of the radiation. Tables 3 and 4 contain numbers related to the saturation point. Complete range of parameters can be traced with plots presented in Figs. 6 and 7. Comparison of these results with those presented in TDR 2006 tells us that decrease of the electron beam emittance (and correspondingly the reduction of the radiation spot size) leads to a significant increase of the angular divergence with respect to previous design.

General features of temporal and spectral structure of the radiation pulses can be traced with Figs. 8 - 13. covering whole range of operating modes with charge from 0.1 nC to 1 nC and wavelength range from 0.1 to 11.6 nm.

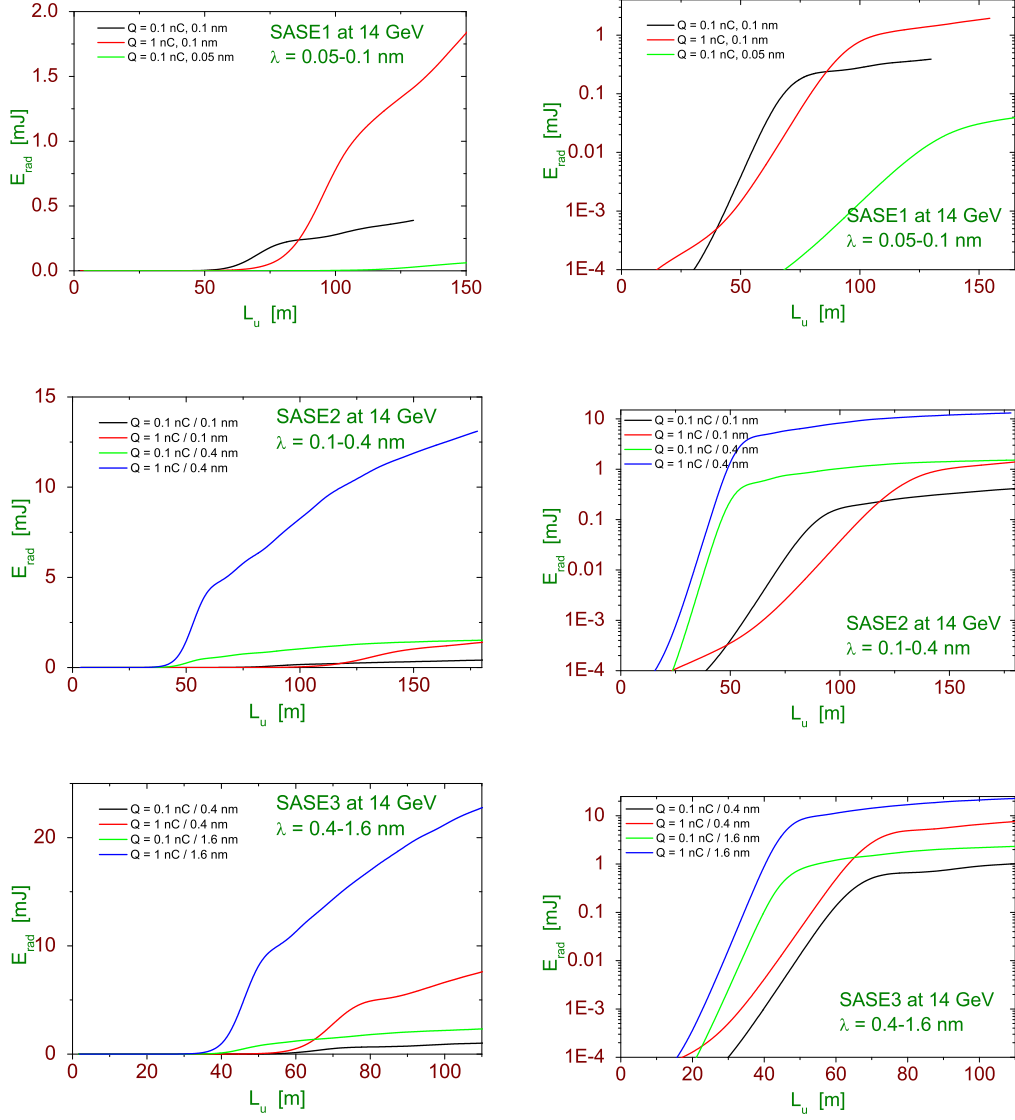


Fig. 5. Energy in the radiation pulse for SASE1, SASE, and SASE3 versus undulator length. Electron beam energy is 14 GeV. Parameters of the electron beam are compiled in Table 1. SASE3 uses "fresh" electron beam. Plots on the left-hand and the right-hand side show linear and logarithmic scale, respectively.

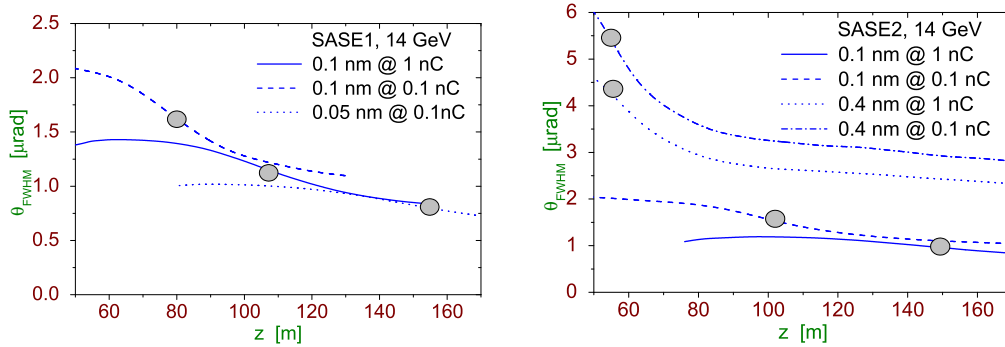


Fig. 6. FWHM angular divergence of the radiation from SASE1 (left plot) and SASE2 (right plot) operating at the energy of 14 GeV. Circles denote saturation point.

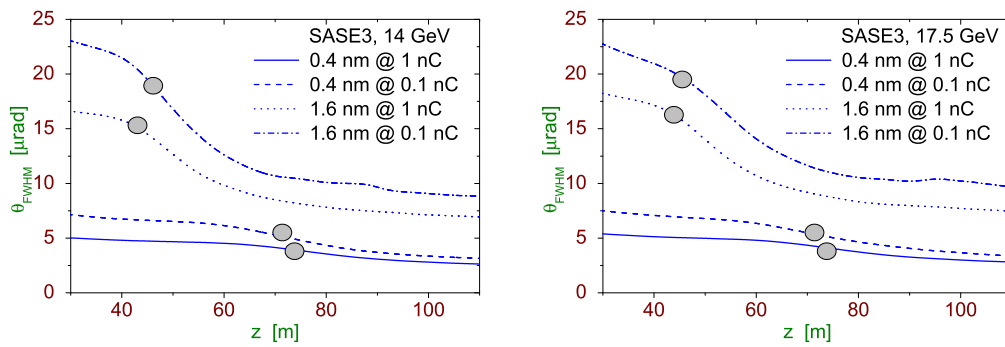


Fig. 7. FWHM angular divergence of the radiation from SASE3 operating at the energy of 14 GeV (left plot) and 17.5 GeV (right plot). Circles denote saturation point.

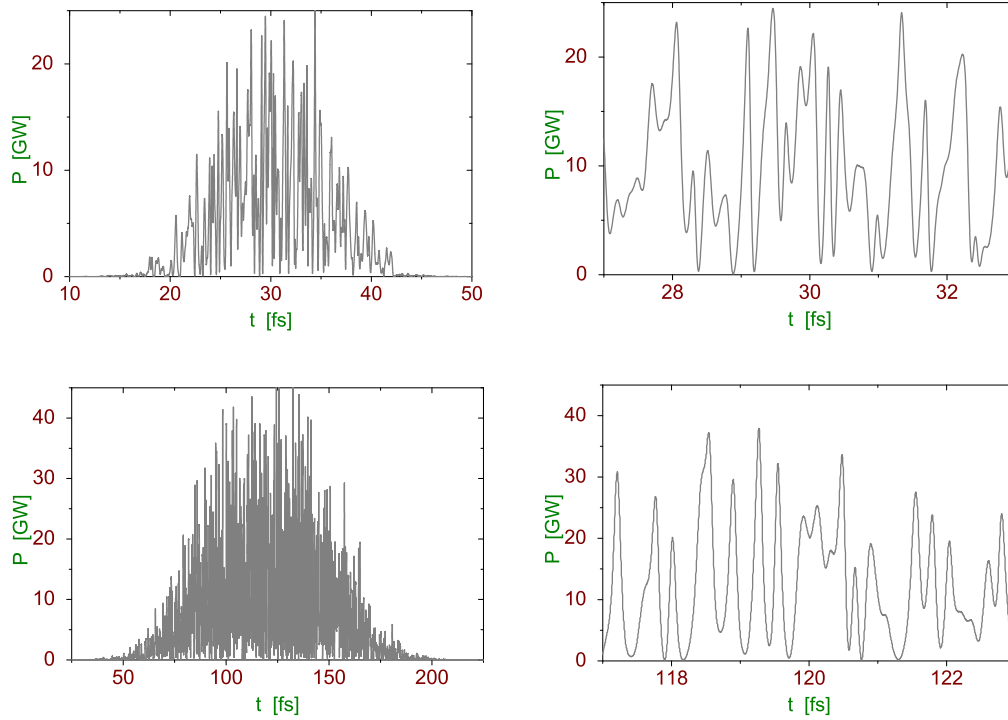


Fig. 8. Temporal structure of the radiation pulse from SASE1 operating in the saturation. Radiation wavelength is equal to 0.1 nm. Energy of the electron beam is equal to 14 GeV. Top plots refer to the bunch charge of 0.1 nC and undulator length of 72 m. Bottom plots refer to the bunch charge of 1 nC and undulator length of 109 m. Plots on the right-hand side present zoomed areas showing fine details. Complete set of the electron beam parameters is presented in Table 1.

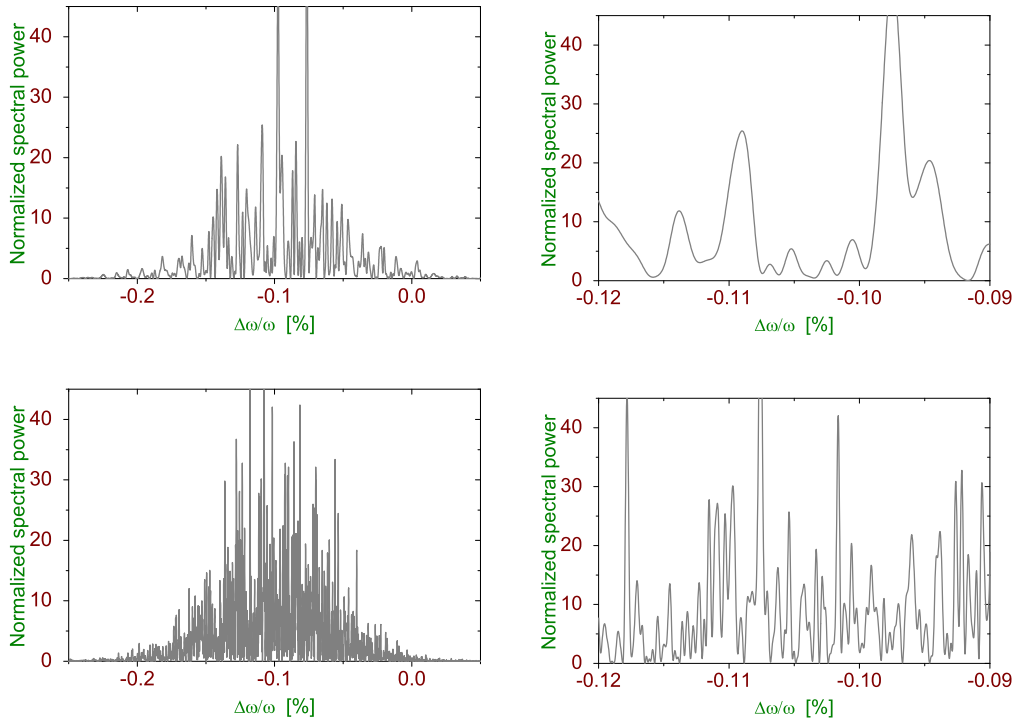


Fig. 9. Spectral structure of the radiation pulse from SASE1 operating in the saturation. Radiation wavelength is equal to 0.1 nm. Energy of the electron beam is equal to 14 GeV. Top plots refer to the bunch charge of 0.1 nC and undulator length of 72 m. Bottom plots refer to the bunch charge of 1 nC and undulator length of 109 m. Plots on the right-hand side present zoomed areas showing fine details. Complete set of the electron beam parameters is presented in Table 1.

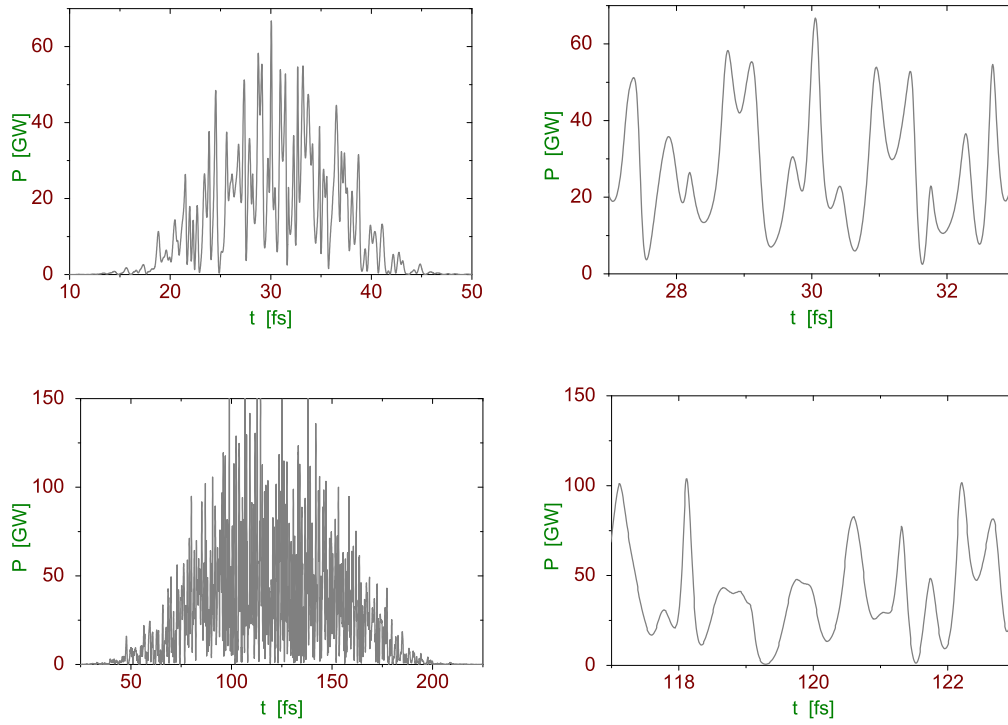


Fig. 10. Temporal structure of the radiation pulse from SASE2 operating in the saturation. Radiation wavelength is equal to 0.4 nm. Energy of the electron beam is equal to 14 GeV. Top plots refer to the bunch charge of 0.1 nC and undulator length of 55 m. Bottom plots refer to the bunch charge of 1 nC and undulator length of 60 m. Plots on the right-hand side present zoomed areas showing fine details. Complete set of the electron beam parameters is presented in Table 1.

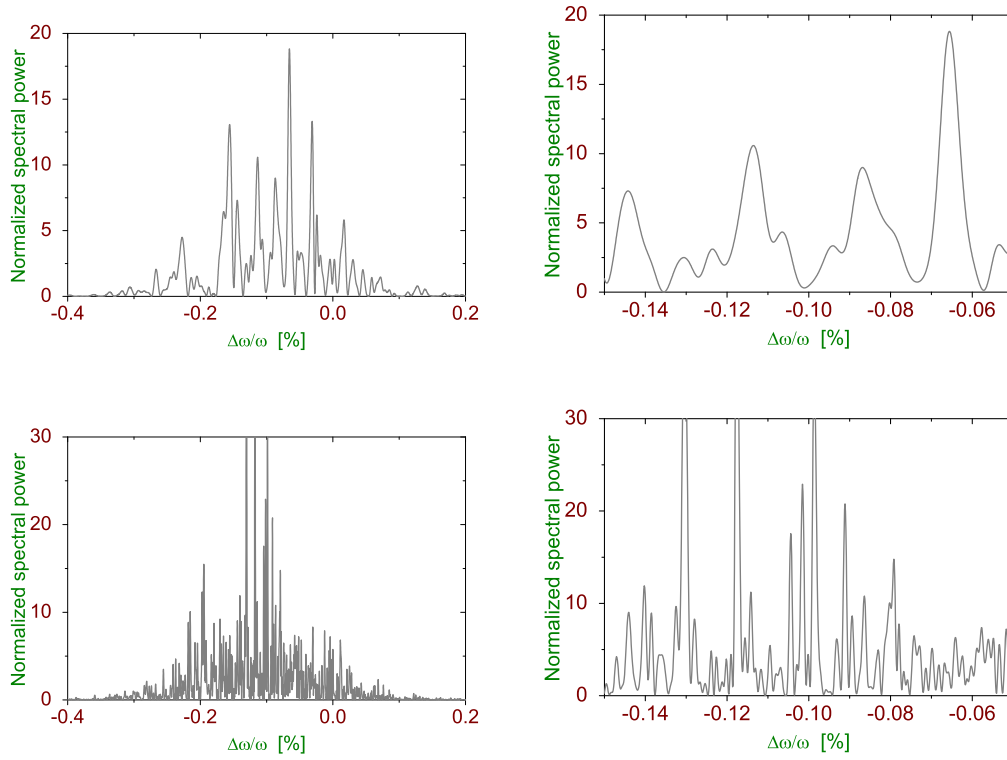


Fig. 11. Spectral structure of the radiation pulse from SASE2 operating in the saturation. Radiation wavelength is equal to 0.4 nm. Energy of the electron beam is equal to 14 GeV. Top plots refer to the bunch charge of 0.1 nC and undulator length of 55 m. Bottom plots refer to the bunch charge of 1 nC and undulator length of 60 m. Plots on the right-hand side present zoomed areas showing fine details. Complete set of the electron beam parameters is presented in Table 1.

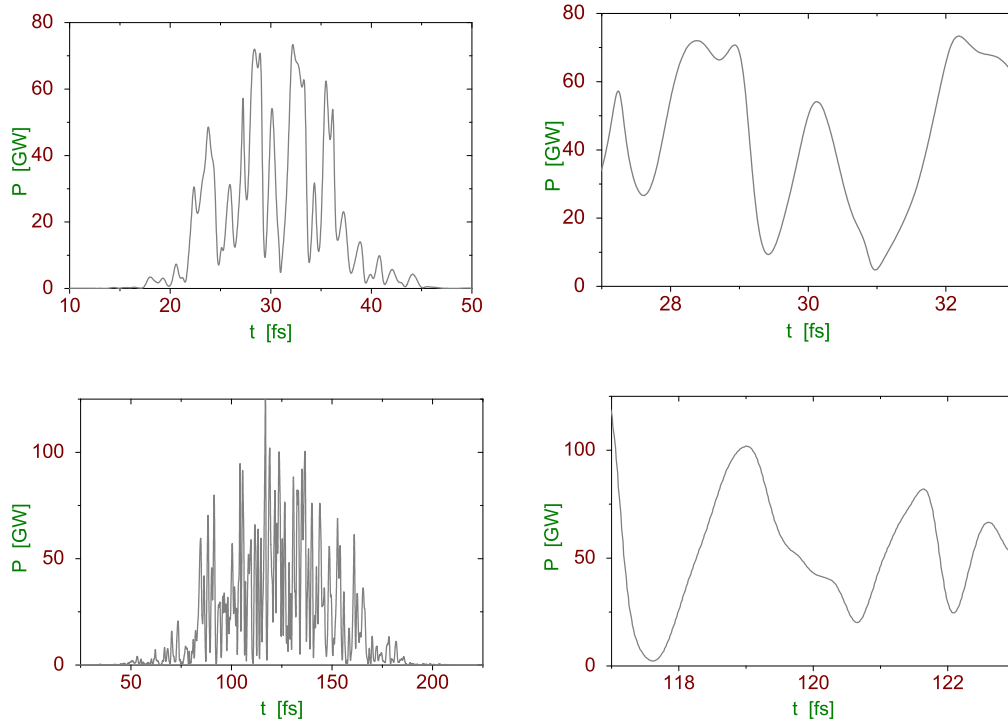


Fig. 12. Temporal structure of the radiation pulse from SASE3 operating in the saturation. Radiation wavelength is equal to 1.6 nm. Energy of the electron beam is equal to 14 GeV. Top plots refer to the bunch charge of 0.1 nC and undulator length of 47 m. Bottom plots refer to the bunch charge of 1 nC and undulator length of 44 m. Plots on the right-hand side present zoomed areas showing fine details. Complete set of the electron beam parameters is presented in Table 1.

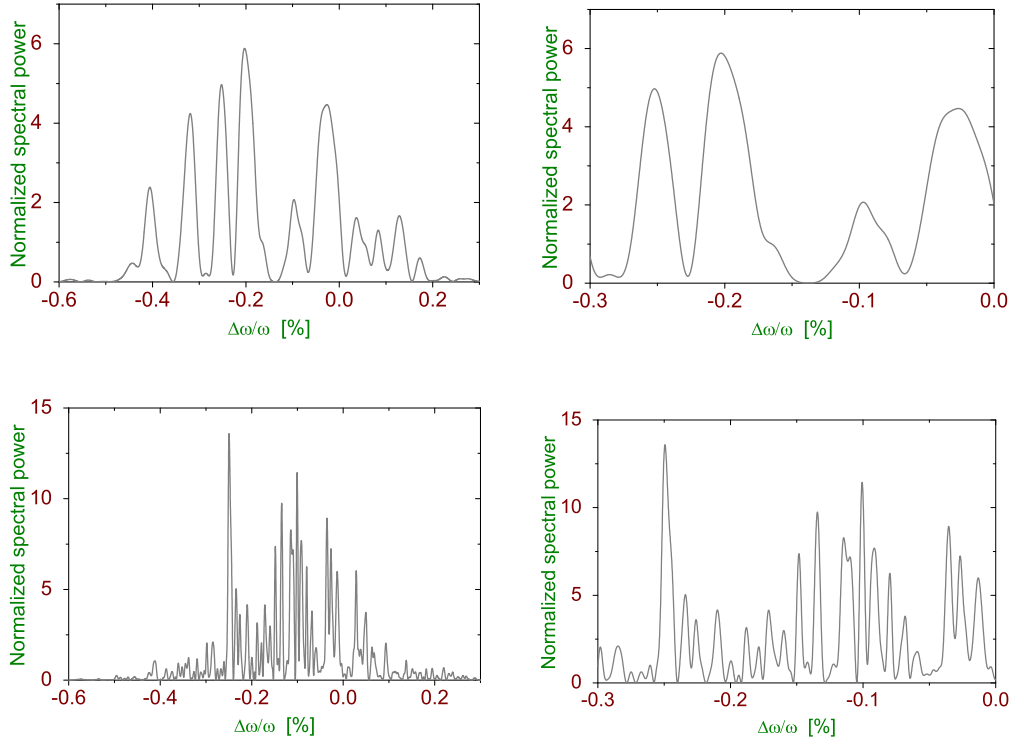


Fig. 13. Spectral structure of the radiation pulse from SASE3 operating in the saturation. Radiation wavelength is equal to 1.6 nm. Energy of the electron beam is equal to 14 GeV. Top plots refer to the bunch charge of 0.1 nC and undulator length of 47 m. Bottom plots refer to the bunch charge of 1 nC and undulator length of 44 m. Plots on the right-hand side present zoomed areas showing fine details. Complete set of the electron beam parameters is presented in Table 1.

Table 3

Specification of photon beam properties for SASE1-SASE3 operating at 14 GeV with new baseline parameters of the electron beam (see Table 1)^a

	Units	SASE1	SASE2	SASE3
Wavelength	nm	0.05	0.1	0.4
Bunch charge	nC	0.1	0.1/1	0.1/1
Photon energy	keV	24.8	12.4	3.1
Energy per pulse	mJ	0.07	0.2/0.9	0.5/4
Peak power	GW	4.4	11/11	27/48
Average power ^b	W	2	5.3/25	12/108
Photon beam size (FWHM)	μm	31	33/49	40/55
Photon beam divergence (FWHM)	μrad	0.9	1.7/1.3	5.2/4
Coherence time	fs	0.18	0.19/0.24	0.39/0.41
Spectrum bandwidth (FWHM) ^c	%	0.06	0.12/0.1	0.24/0.23
Degree of transverse coherence		0.78	0.95/0.66	0.95/0.95
Pulse duration (FWHM)	fs	17	17/84	17/84
Number of photons per pulse	10^{12}	0.018	0.1/0.5	0.9/8
Average flux of photons ^b	10^{16}	0.05	0.26/1.3	0.24/1.2
Peak brilliance	$\text{B}/10^{33}$	2.1	1.8/1.5	1.7/1.5
Average brilliance ^b	$\text{B}/10^{24}$	1.	1.7/3.4	0.76/3.4
Saturation length ^d	m	158	72/108	99/149
			51/54	66/72
				45/44

^aCharacteristics of the photon beam are calculated in the saturation regime for charges of 0.1 nC and 1 nC (relevant numbers are separated by slash).

^bAveraged characteristics are calculated for 27000 pulses per second (10 Hz, 2700 pulses per macropulse).

^cNatural FEL bandwidth without effect of energy chirp in the electron beam.

^dFEL parameters are optimized for minimum saturation length. The lower limit for undulator beta-function is 15 m.

Table 4

Specification of photon beam properties for SASE3 operating in saturation at 14 GeV and 17.5 GeV with new baseline parameters of the electron beam (see Table 1)^a

	Units	14 GeV	17.5 GeV
Wavelength	nm	0.4	1.6
Bunch charge	nC	0.1/1	0.1/1
Photon energy	keV	3.1	0.8
Energy per pulse	mJ	0.5/4.	0.7/7.
Peak power	GW	28/48	44/90
Average power ^b	W	13/109	20/200
Photon beam size (FWHM)	μm	42/48	48/67
Photon beam divergence (FWHM)	μrad	4.8/3.8	14/12
Coherence time	fs	0.36/0.39	1/0.9
Spectrum bandwidth (FWHM) ^c	%	0.26/0.24	0.39/0.4
Pulse duration (FWHM)	fs	17/84	17/84
Number of photons per pulse	10^{12}	1/8	6/60
Average flux of photons ^b	10^{16}	2.6/22	16/160
Peak brilliance	B/ 10^{33}	0.5/0.9	0.14/0.27
Average brilliance ^b	B/ 10^{24}	0.24/2.1	0.06/0.6
Saturation length ^d	m	66/72	45/44
			67/72
			47/45

^aCharacteristics of the photon beam are calculated in the saturation regime for charges of 0.1 nC and 1 nC (relevant numbers are separated by slash).

^bAveraged characteristics are calculated for 27000 pulses per second (10 Hz, 2700 pulses per macropulse).

^cNatural FEL bandwidth without effect of energy chirp in the electron beam.

^dFEL parameters are optimized for minimum saturation length.

The lower limit for undulator beta-function is 15 m.

Table 5
 Specification of photon beam properties for SASE1-SASE3
 / Baseline parameters of EXFEL TDR 2006 [6] /

	Units	SASE1	SASE2	SASE3
Wavelength range	nm	0.1	0.1-0.4	0.4-1.6
Photon energy range	keV	12.4	12.4-3.1	3.1-0.8
Peak power	GW	20	20-80	80-130
Average power	W	65	65-260	260-420
Photon beam size (FWHM)	μm	70	85-55	60-70
Photon beam divergence (FWHM)	μrad	1	0.84-3.4	3.4-11.4
Coherence time	fs	0.2	0.22-0.38	0.34-0.88
Spectrum bandwidth (FWHM)	%	0.08	0.08-0.18	0.2-0.3
Pulse duration (FWHM)	fs	100	100	100
Number of photons per pulse	#	10^{12}	$10^{12} - 1.6 \times 10^{13}$	$1.6 \times 10^{13} - 10^{14}$
Average flux of photons	#/sec	3.3×10^{16}	$3.3 \times 10^{16} - 5.2 \times 10^{17}$	$5.2 \times 10^{17} - 3.4 \times 10^{18}$
Peak brilliance	B	5×10^{33}	$5 \times 10^{33} - 2.2 \times 10^{33}$	$2 \times 10^{33} - 5 \times 10^{32}$
Average brilliance	B	1.6×10^{25}	$1.6 \times 10^{25} - 7.1 \times 10^{24}$	$6.4 \times 10^{24} - 1.6 \times 10^{24}$

Table 6

Comparative table of the properties of the radiation from SASE1 operating in the saturation regime for three different scenario:

i) parameters of electron beam from TDR 2006 [6] and energy 17.5 GeV;

ii) new parameters of the electron beam [3] and energy 17.5 GeV;

iii) new parameters of the electron beam [3] and energy 14 GeV*

	Units	2006 / 17.5 GeV	2010 / 17.5 GeV	2010 / 14 GeV
Electron energy	GeV	17.5	17.5	14
Bunch charge	nC	1	1	1
Peak beam current	A	5000	5000	5000
Normalized rms emittance	mm-mrad	1.4	1.05	1.05
rms energy spread	MeV	1	2	2
Wavelength	nm	0.1	0.1	0.1
Photon energy	keV	12.4	12.4	12.4
Energy per pulse	mJ	1.	1.3	0.9
Peak power	GW	11.7	15.6	11
Average power	W	27	35	25
Coherence time	fs	0.28	0.22	0.24
Degree of transverse coherence		0.62	0.78	0.66
Number of photons per pulse	10^{12}	0.5	0.7	0.5
Average flux of photons	10^{16}	1.3	1.8	1.3
Peak brilliance	$B/10^{33}$	1.6	2.1	1.4
Average brilliance	$B/10^{24}$	3.8	5.1	3.4
Saturation length	m	124	97	108

* Averaged characteristics are calculated for 27000 pulses per second. The same rms length of electron bunch of 60 fs is used in all cases to simplify comparison of the radiation properties.

5 An overview of saturation properties of SASE1

In this section we present detailed overview of saturation characteristics of SASE1 in the range of operating charges 0.1 - 1 nC and operating energies of 14 GeV and 17.5 GeV. All results are presented on a two dimensional plane. Horizontal axis is operating charge. All other parameters of the electron beam are compiled in Table 1. Vertical axis is operating wavelength. Maximum wavelength is defined by minimum undulator gap, and is equal to 0.156 nm and 0.1 nm for the energy of electrons of 14 GeV and 17.5 GeV, respectively. Dashed red line denotes lower boundary of reachable wavelength range. It is defined by the length of the undulator of 165 meters.

Application of similarity techniques to the results of numerical simulations allows to define general parametric dependencies of the saturation characteristics of SASE FEL. Relevant studies have been performed in paper [12] in approximation of small energy spread. Application of these formulae gives approximate description of the saturation characteristics in the whole range of operating charges. An important conclusion is that peak power and peak brilliance of SASE1/SASE2 operating around 0.1nm depend rather weakly on the bunch charge. On the other hand, average brilliance and average photon flux increase significantly with the bunch charge. Another conclusion is that operation at high charge will result in the visible decrease of the degree of transverse coherence.

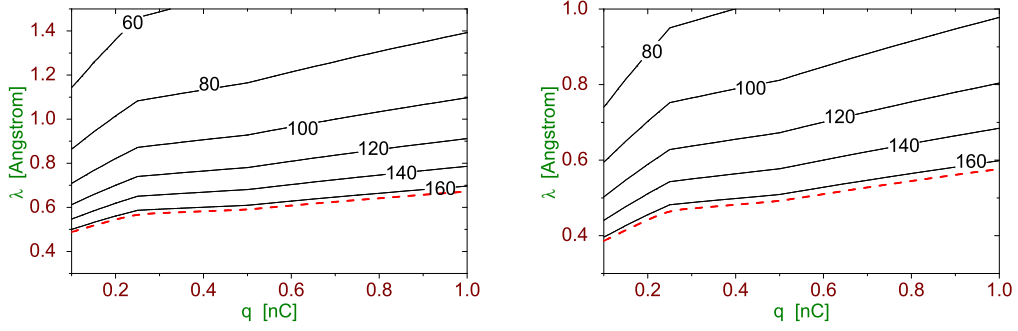


Fig. 14. Saturation length for SASE1 versus bunch charge and operating wavelength. Plots on the left hand side and the right hand side correspond to the electron energy of 14 GeV and 17.5 GeV, respectively. Parameters of SASE1 are optimized for minimum gain length.

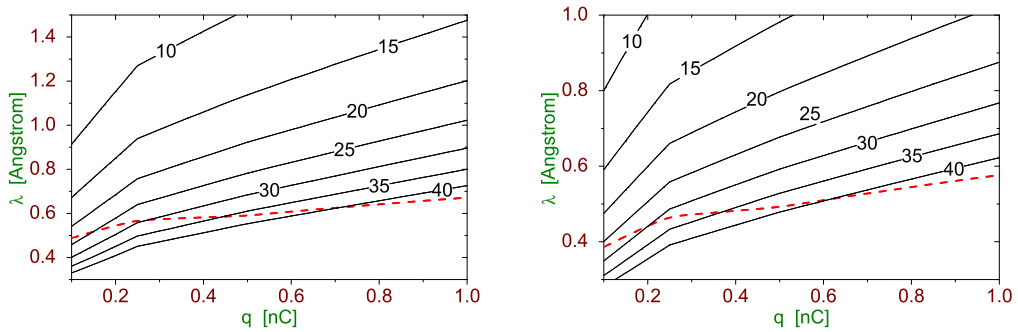


Fig. 15. Optimum focusing beta function for SASE1 versus bunch charge and operating wavelength. Plots on the left hand side and the right hand side correspond to the electron energy of 14 GeV and 17.5 GeV, respectively. Parameters of SASE1 are optimized for minimum gain length.

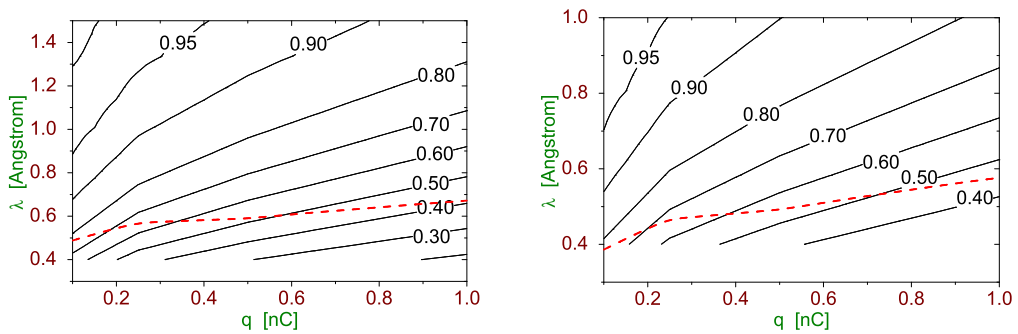


Fig. 16. Degree of transverse coherence of the radiation from SASE1 operating in the saturation versus bunch charge and operating wavelength. Plots on the left hand side and the right hand side correspond to the electron energy of 14 GeV and 17.5 GeV, respectively. Parameters of SASE1 are optimized for minimum gain length.

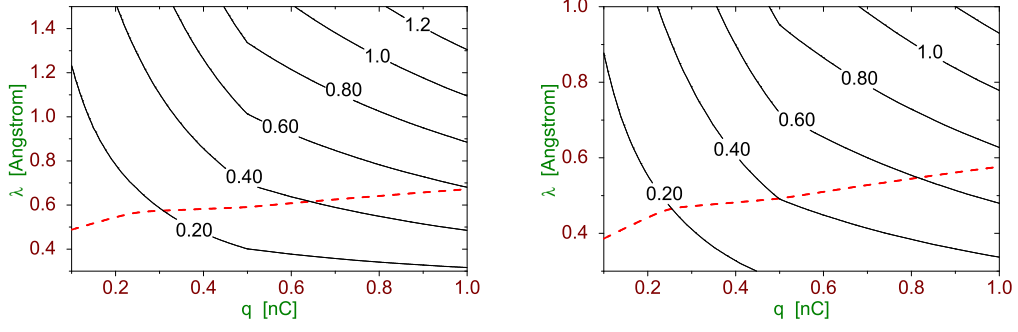


Fig. 17. Pulse energy of the radiation from SASE1 operating in the saturation versus bunch charge and operating wavelength. Plots on the left hand side and the right hand side correspond to the electron energy of 14 GeV and 17.5 GeV, respectively. Parameters of SASE1 are optimized for minimum gain length.

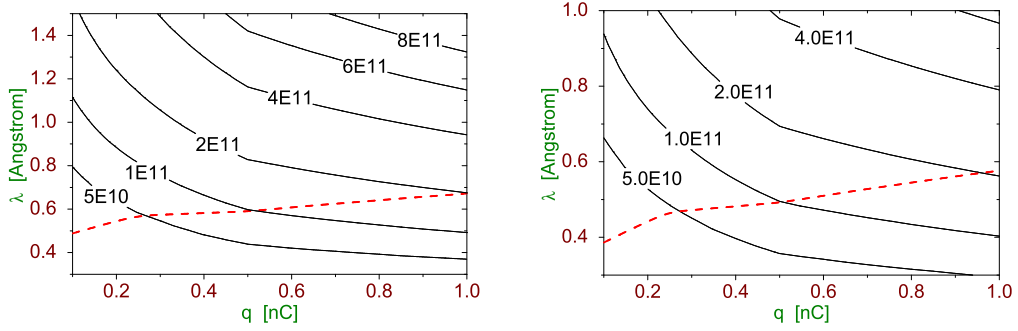


Fig. 18. Number of photons in the radiation pulse from SASE1 operating in the saturation versus bunch charge and operating wavelength. Plots on the left hand side and the right hand side correspond to the electron energy of 14 GeV and 17.5 GeV, respectively. Parameters of SASE1 are optimized for minimum gain length.

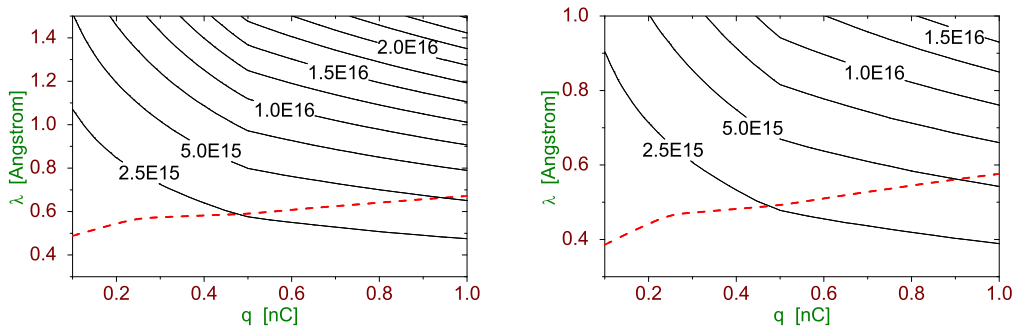


Fig. 19. Average photon flux (in units of *photons/sec*) from SASE1 operating in the saturation versus bunch charge and operating wavelength. Plots on the left hand side and the right hand side correspond to the electron energy of 14 GeV and 17.5 GeV, respectively. Parameters of SASE1 are optimized for minimum gain length.

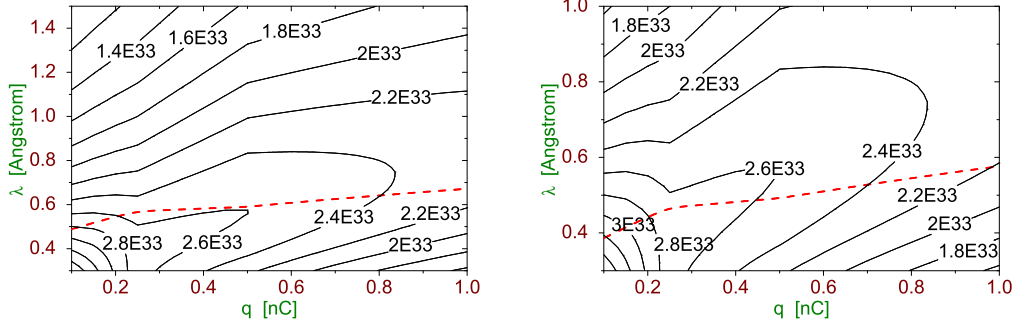


Fig. 20. Peak brilliance of the radiation from SASE1 operating in the saturation versus bunch charge and operating wavelength. Plots on the left hand side and the right hand side correspond to the electron energy of 14 GeV and 17.5 GeV, respectively. Parameters of SASE1 are optimized for minimum gain length.

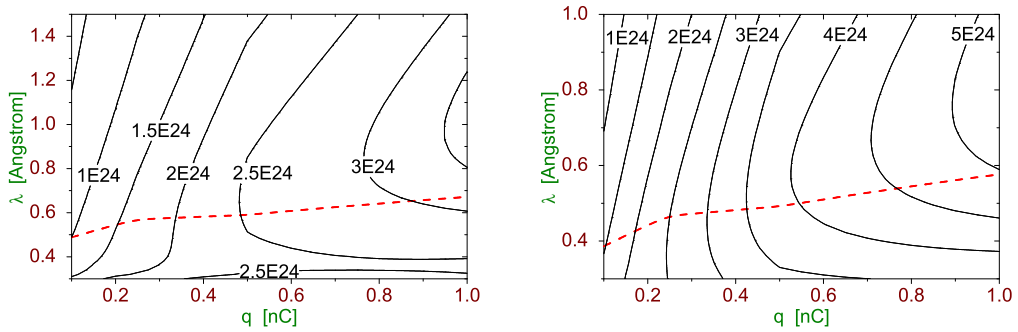


Fig. 21. Average brilliance of the radiation from SASE1 operating in the saturation versus bunch charge and operating wavelength. Plots on the left hand side and the right hand side correspond to the electron energy of 14 GeV and 17.5 GeV, respectively. Parameters of SASE1 are optimized for minimum gain length.

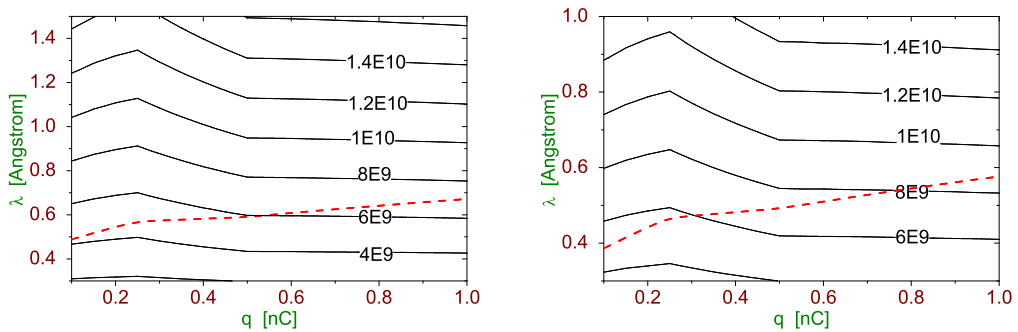


Fig. 22. Peak power of the radiation (in units of W) from SASE1 operating in the saturation versus bunch charge and operating wavelength. Plots on the left hand side and the right hand side correspond to the electron energy of 14 GeV and 17.5 GeV, respectively. Parameters of SASE1 are optimized for minimum gain length.

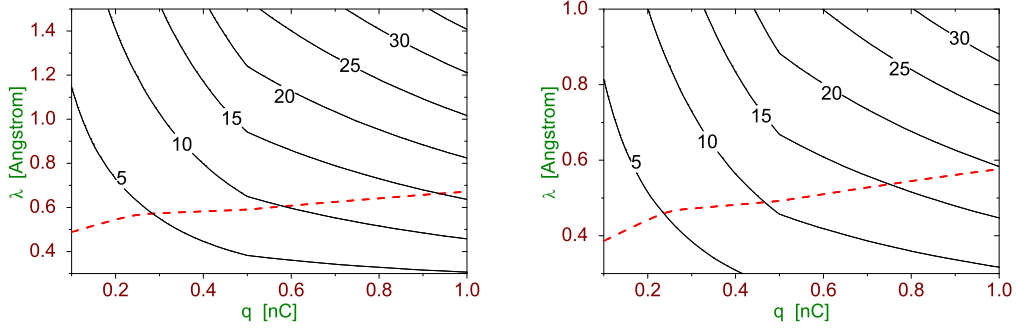


Fig. 23. Average power of the radiation (in units of W) from SASE1 operating in the saturation versus bunch charge and operating wavelength. Plots on the left hand side and the right hand side correspond to the electron energy of 14 GeV and 17.5 GeV, respectively. Parameters of SASE1 are optimized for minimum gain length.

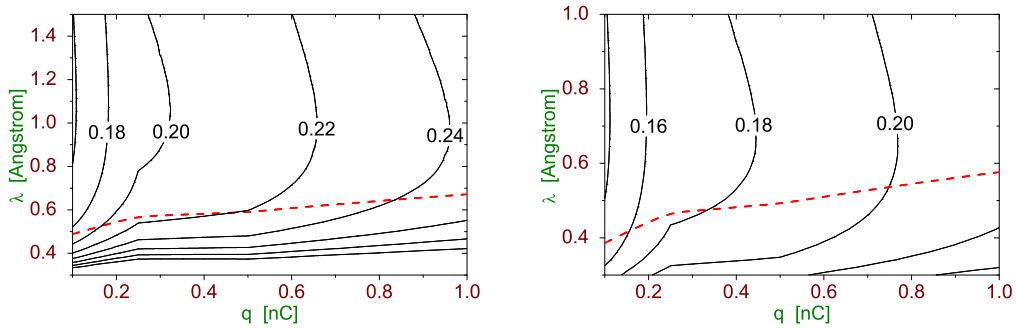


Fig. 24. Coherence time of the radiation (in units of fs) from SASE1 operating in the saturation versus bunch charge and operating wavelength. Plots on the left hand side and the right hand side correspond to the electron energy of 14 GeV and 17.5 GeV, respectively. Parameters of SASE1 are optimized for minimum gain length.

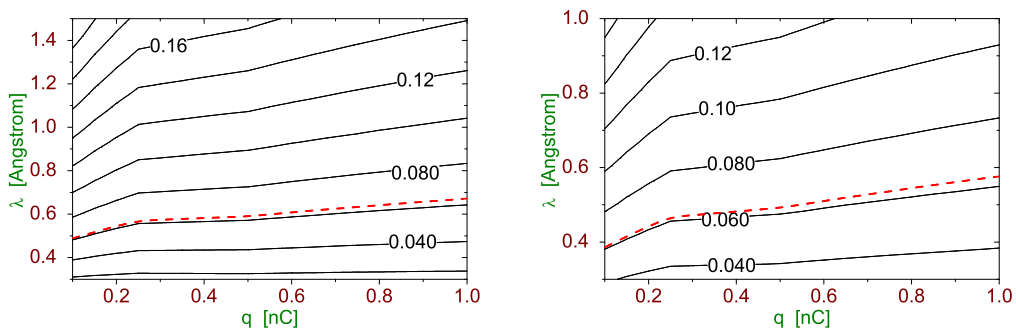


Fig. 25. FWHM bandwidth of the radiation (in units of %) from SASE1 operating in the saturation versus bunch charge and operating wavelength. Plots on the left hand side and the right hand side correspond to the electron energy of 14 GeV and 17.5 GeV, respectively. Parameters of SASE1 are optimized for minimum gain length.

6 Operation of SASE3 as an afterburner

With new parameter set for the electron beam presented in Table 1 there are a lot of possible tuning of the amplification process in SASE1. Different tuning provide different energy spread in the electron beam as it is illustrated in Fig. 26. Energy of the electron beam can be also different. Three options for the electron beam energy are under discussion at the moment: 17.5 GeV, 14 GeV, and 10 GeV. Thus, operation of SASE3 as an afterburner becomes to be rather tricky.

Figure 4 shows the dependence of minimum wavelength in SASE3 on bunch charge and energy spread in the electron beam. We see that minimum wavelength increases with the energy spread in the electron beam. Operation at 17.5 GeV is a bit less sensitive to the energy spread with respect to 14 GeV working point. One should care about control of the amplification process in SASE1 in order to avoid deep nonlinear regime leading to large energy spread when operating SASE3 at short wavelengths. Operation of SASE3 at long wavelengths is less sensitive to the energy spread and can be decoupled from the mode of SASE1 operation. Dependence of minimum wavelength in SASE3 on the bunch charge is rather weak. On the other hand, energy spread in the electron beam induced by the SASE process in the SASE1 undulator is less for higher charges. Thus, mode of operation with higher charge can provide wider possibilities for decoupling users of SASE1 and SASE3. Operation of SASE1 at shorter wavelength also helps to decouple SASE3 operation.

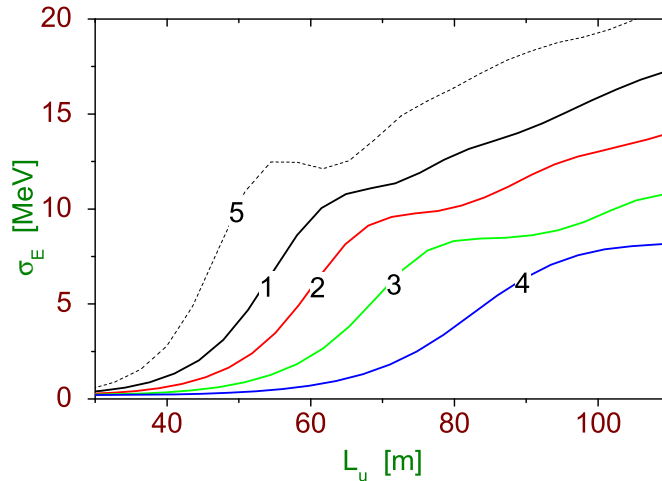


Fig. 26. Energy spread in the electron beam along undulator length in SASE1. Energy of the electron beam is equal to 14 GeV. Curves 1, 2, 3, and 4 show the case of operating wavelength of 0.1 nm for different charges 0.1 nC, 0.25 nC, 0.5 nC, and 1 nC, respectively. Curve 5 shows the case of operating wavelength of 0.15 nm and bunch charge of 0.1 nC.

7 Design formulae for an optimized XFEL

Design of the focusing system of XFEL assumes nearly uniform focusing of the electron beam in the undulator, so we consider axisymmetric model of the electron beam. It is assumed that transverse distribution function of the electron beam is Gaussian, so rms transverse size of matched beam is $\sigma = \sqrt{\epsilon\beta}$, where $\epsilon = \epsilon_n/\gamma$ is rms beam emittance, γ is relativistic factor, and β is focusing beta-function. An important feature of the parameter space of XFEL is that the space charge field does not influence significantly on the FEL process and calculation of the FEL process can be performed by taking into account diffraction effects, the energy spread in the electron beam, and effects of betatron motion only. In the framework of the three-dimensional theory operation of the FEL amplifier is described by the following parameters: the diffraction parameter B , the energy spread parameter $\hat{\Lambda}_T^2$, and the betatron motion parameter \hat{k}_β [15, 18]:

$$\begin{aligned} B &= 2\Gamma\sigma^2\omega/c, \\ \hat{k}_\beta &= 1/(\beta\Gamma), \\ \hat{\Lambda}_T^2 &= (\sigma_E/\mathcal{E})^2/\rho^2, \end{aligned} \tag{8}$$

where $\Gamma = [I\omega^2\theta_s^2 A_{JJ}^2/(I_A c^2 \gamma_z^2 \gamma)]^{1/2}$ is the gain parameter and $\rho = c\gamma_z^2\Gamma/\omega$ is the efficiency parameter. When describing shot noise in the electron beam, one more parameter appears, the number of electrons on the coherence length, $N_c = I/(e\omega\rho)$. The following notations are used here: I is the beam current, $\omega = 2\pi c/\lambda$ is the frequency of the electromagnetic wave, $\theta_s = K_{\text{rms}}/\gamma$, K_{rms} is the rms undulator parameter, $\gamma_z^{-2} = \gamma^{-2} + \theta_s^2$, $k_w = 2\pi/\lambda_w$ is the undulator wavenumber, $I_A = 17$ kA is the Alfvén current, $A_{JJ} = 1$ for helical undulator and $A_{JJ} = J_0(K_{\text{rms}}^2/2(1 + K_{\text{rms}}^2)) - J_1(K_{\text{rms}}^2/2(1 + K_{\text{rms}}^2))$ for planar undulator. Here J_0 and J_1 are the Bessel functions of the first kind. The energy spread is assumed to be Gaussian with rms deviation σ_E .

The amplification process in the FEL amplifier passes two stages, linear and nonlinear. The linear stage lasts over significant fraction of the undulator length (about 80%), and the main target for XFEL optimization is the field gain length. In the linear high-gain limit the radiation emitted by the electron beam in the undulator can be represented as a set of modes [19–21]:

$$E_x + iE_y = \int d\omega \exp[i\omega(z/c - t)] \times \sum_{n,m} A_{nm}(\omega, z) \Phi_{nm}(r, \omega) \exp[\Lambda_{nm}(\omega)z + in\phi] \tag{9}$$

When amplification takes place, the mode configuration in the transverse plane

remains unchanged while the amplitude grows exponentially with the undulator length. Each mode is characterized by the eigenvalue $\Lambda_{nm}(\omega)$ and the field distribution eigenfunction $\Phi_{nm}(r, \omega)$ in terms of transverse coordinates. At sufficient undulator length fundamental TEM₀₀ mode begins to give main contribution to the total radiation power. Thus, relevant value of interest for XFEL optimization is the field gain length of the fundamental mode, $L_g = 1/\text{Re}(\Lambda_{00})$, which gives good estimate for expected length of the undulator needed to reach saturation, $L_{\text{sat}} \simeq 10 \times L_g$. Optimization of the field gain length is performed by means of numerical solution of the corresponding eigenvalue equations taking into account all the effects (diffraction, energy spread and emittance) [18, 22, 23]. Computational possibilities of modern computers allows to trace complete parameter space of XFEL (which in fact is 11-dimensional). From practical point of view it is important to find an absolute minimum of the gain length corresponding to optimum focusing beta function. For this practically important case the solution of the eigenvalue equation for the field gain length of the fundamental mode and optimum beta function are rather accurately approximated by [24]:

$$\begin{aligned} L_g &= 1.67 \left(\frac{I_A}{I} \right)^{1/2} \frac{(\epsilon_n \lambda_w)^{5/6}}{\lambda^{2/3}} \frac{(1 + K^2)^{1/3}}{K A_{JJ}} (1 + \delta), \\ \beta_{\text{opt}} &\simeq 11.2 \left(\frac{I_A}{I} \right)^{1/2} \frac{\epsilon_n^{3/2} \lambda_w^{1/2}}{\lambda K A_{JJ}} (1 + 8\delta)^{-1/3}, \\ \delta &= 131 \frac{I_A}{I} \frac{\epsilon_n^{5/4}}{\lambda^{1/8} \lambda_w^{9/8}} \frac{\sigma_\gamma^2}{(K A_{JJ})^2 (1 + K^2)^{1/8}}, \end{aligned} \quad (10)$$

where $\sigma_\gamma = \sigma_E/m_e c^2$. Accuracy of this fit is better than 5% in the range of parameter $\hat{\epsilon} = 2\pi\epsilon/\lambda$ from 1 to 5.

Equation (10) demonstrates clear interdependence of physical parameters defining operation of the XFEL. Let us consider the case of negligibly small energy spread. Under this condition diffraction parameter B and parameter of betatron oscillations, \hat{k}_β are functions of the only parameter $\hat{\epsilon}$:

$$B \simeq 12.5 \times \hat{\epsilon}^{5/2}, \quad \hat{k}_\beta = 1/(\beta\Gamma) \simeq 0.158/\hat{\epsilon}^{3/2}. \quad (11)$$

FEL equations written down in the dimensionless form involve an additional parameter N_c defining the initial conditions for the start-up from the shot noise. Note that the dependence of output characteristics of the SASE FEL operating in saturation is slow, in fact logarithmic in terms of N_c . Thus, we can conclude that with logarithmic accuracy in terms of N_c , characteristics of the SASE FEL written down in a normalized form are functions of the only parameter $\hat{\epsilon}$.

In Fig. 1 we present evolution of the main characteristics of a SASE FEL along the undulator. If one traces evolution of the brilliance (degeneracy parameter) of

the radiation along the undulator length, there is always the point (defined as the saturation point [10]) where the brilliance reaches maximum value. The best properties of the radiation in terms of transverse and longitudinal coherence are reached just before the saturation point, and then degrade significantly despite the radiation power continuing to grow with the undulator length.

Application of similarity techniques allows us to derive universal parametric dependencies of the output characteristics of the radiation at the saturation point. As we mentioned in Section 2, within accepted approximations (optimized SASE FEL and negligibly small energy spread in the electron beam), normalized output characteristics of a SASE FEL at the saturation point are functions of only two parameters: $\hat{\epsilon} = 2\pi\epsilon/\lambda$ and the number of electrons in the volume of coherence $N_c = IN_g\lambda/c$, where $N_g = L_g/\lambda_w$ is the number of undulator periods per gain length. Characteristics of practical interest are: saturation length L_{sat} , saturation efficiency $\eta_{\text{sat}} = P_{\text{sat}}/P_b$ (ratio of the radiation power to the electron beam power $P_b = \gamma mc^2 I/e$), coherence time τ_c , degree of transverse coherence ζ , degeneracy parameter δ , and brilliance B_r . Applications of similarity techniques to the results of numerical simulations of a SASE FEL [10] gives us the following result [12]:

$$\begin{aligned}
\hat{L}_{\text{sat}} &= \Gamma L_{\text{sat}} \simeq 2.5 \times \hat{\epsilon}^{5/6} \times \ln N_c , \\
\hat{\eta} &= P/(\bar{\rho}P_b) \simeq 0.17/\hat{\epsilon} , \\
\hat{\tau}_c &= \bar{\rho}\omega\tau_c \simeq 1.16 \times \sqrt{\ln N_c} \times \hat{\epsilon}^{5/6} , \\
\sigma_\omega &= \sqrt{\pi}/\tau_c .
\end{aligned} \tag{12}$$

These expressions provide reasonable practical accuracy for $\hat{\epsilon} \gtrsim 0.5$. With logarithmic accuracy in terms of N_c characteristics of the SASE FEL expressed in a normalized form are functions of the only parameter $\hat{\epsilon}$. The saturation length, FEL efficiency, and coherence time exhibit monotonous behavior in the parameter space of modern XFELs ($\hat{\epsilon} \simeq 0.5 \dots 5$). Situation is a bit complicated with the degree of transverse coherence as one can see in Fig. 28. The degree of transverse coherence reaches a maximum value in the range of $\hat{\epsilon} \sim 1$, and drops at small and large values of $\hat{\epsilon}$. At small values of the emittance, the degree of transverse coherence is limited by the interdependence of poor longitudinal coherence and transverse coherence [25]. Due to the start-up from shot noise, every radiation mode entering eq. (9) is excited within finite spectral bandwidth. This means that the radiation from a SASE FEL is formed by many fundamental TEM_{00} modes with different frequencies. The transverse distribution of the radiation field of the mode is also different for different frequencies. Smaller values of $\hat{\epsilon}$ (smaller value of the diffraction parameter) correspond to larger frequency bandwidths. This effect explains the decrease of the transverse coherence at small values of $\hat{\epsilon}$. The degree of transverse coherence asymptotically approaches unity as $(1 - \zeta) \propto 1/z \propto 1/\ln N_c$ at small values of the emittance.

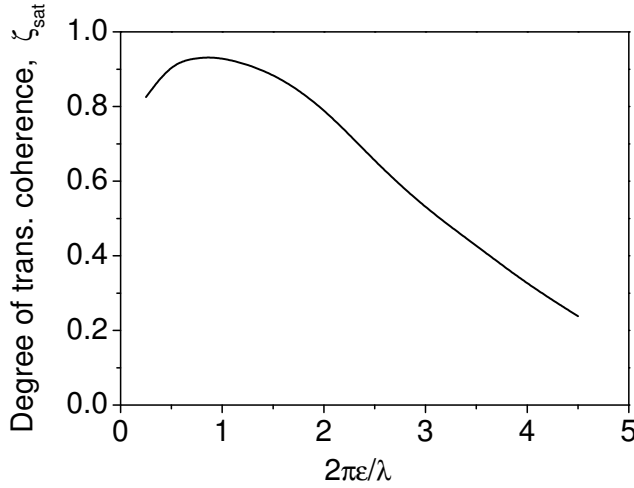


Fig. 28. Degree of transverse coherence, ζ_{sat} in the saturation versus parameter $\hat{\epsilon}$.

In the case of large emittance the degree of transverse coherence is defined by the contents of higher transverse modes [10, 11]. When $\hat{\epsilon}$ increases, the diffraction parameter increases as well, leading to the degeneration of the radiation modes [15]. The amplification process in the SASE FEL passes limited number of the field gain lengths, and starting from some value of $\hat{\epsilon}$, the linear stage of amplification becomes too short to provide a mode selection process (9). When the amplification process enters the nonlinear stage, the mode content of the radiation becomes richer due to independent growth of the radiation modes in the nonlinear medium. Thus, at large values of $\hat{\epsilon}$ the degree of transverse coherence is limited by poor mode selection. The degree of transverse coherence scales as $\zeta_{\text{sat}} \propto (\ln N_c / \hat{\epsilon})^2$ in the asymptote of large emittance. To avoid complications, we present here just a fit for the degree of transverse coherence for the number of electrons in the coherence volume $N_c = 4 \times 10^6$:

$$\zeta_{\text{sat}} \simeq \frac{1.1\hat{\epsilon}^{1/4}}{1 + 0.15\hat{\epsilon}^{9/4}}. \quad (13)$$

Recalculation from reduced to dimensional parameters is straightforward. For instance, saturation length is $L_{\text{sat}} \simeq 0.6 \times L_g \times \ln N_c$. Using (12) and (13) we can calculate normalized degeneracy parameter $\hat{\delta} = \hat{\eta}\zeta\hat{\tau}_c$ and then the brilliance (5):

$$B_r \left[\frac{\text{photons}}{\text{sec mrad}^2 \text{ mm}^2 \text{ 0.1\% bandw.}} \right] \simeq 4.5 \times 10^{31} \times \frac{I[\text{kA}] \times E[\text{GeV}]}{\lambda[\text{\AA}]} \times \hat{\delta}. \quad (14)$$

References

- [1] I. Zagorodnov and M. Dohlus, A Semi-Analytical Modelling of Multistage Bunch Compression with Collective Effects, Preprint DESY 10-102, DESY, Hamburg, 2010.
- [2] I. Zagorodnov, Ultra-Short Low Charge Operation at FLASH and the European XFEL, Proc. FEL 2010 Conference, WEOBI2.
- [3] Data by T. Limberg and W. Decking by April 12, 2010 present approximation of the results of start-to-end-simulation for lasing fraction of the beam in terms of gaussian beam with uniform along the bunch emittance and energy spread. Inconsistency of rms bunch charge, peak current, and rms pulse width resolved by an assumption that non-gaussian tails (about 20% of the bunch charge) do not contribute to the lasing process. Note that such simplified model predicts only natural FEL bandwidth of the radiation ignoring chirp of energy in the electron beam.
- [4] P. Emma et al., First lasing and operation of an Angstrom-wavelength free-electron laser, *Nature Photonics* 4, 641-647 (2010).
- [5] J. Arthur et al., Linac Coherent Light Source (LCLS), Conceptual Design Report, SLAC-R593 (SLAC, Stanford 2002)
(see also <http://www-ssrl.slac.stanford.edu/lcls/cdr>).
- [6] M. Altarelli et al. (Eds.), XFEL: The European X-Ray Free-Electron Laser. Technical Design Report, Preprint DESY 2006-097, DESY, Hamburg, 2006 (see also <http://xfel.desy.de>).
- [7] W. Ackermann et al., Operation of a free electron laser from the extreme ultraviolet to the water window, *Nature Photonics* 1, 336-342 (2007).
- [8] S. Rimjaem et al., Proc. IPAC'10 Conference, TUPE011.
- [9] S. Rimjaem et al., Proc. FEL 2010 Conference, WEPB09.
- [10] E.L. Saldin, E.A. Schneidmiller, and M.V. Yurkov, *Opt. Commun.* 281(2008)1179.
- [11] E.L. Saldin, E.A. Schneidmiller, and M.V. Yurkov, *Opt. Commun.* 281(2008)4727.
- [12] E.L. Saldin, E.A. Schneidmiller, and M.V. Yurkov, *New J. Phys.* 12 (2010) 035010.
- [13] E.L. Saldin, E.A. Schneidmiller and M.V. Yurkov, "FAST: a three-dimensional time-dependent FEL simulation code", *Nucl. Instrum. and Methods* **A429**(1999)233–237.
- [14] J. Goodman, *Statistical Optics*, (John Wiley and Sons, New York, 1985).
- [15] E.L. Saldin, E.A. Schneidmiller, M.V. Yurkov, "The Physics of Free Electron Lasers" (Springer-Verlag, Berlin, 1999).
- [16] J. Pflueger (European XFEL), private communication.
- [17] R. Brinkmann, E.A. Schneidmiller, M.V. Yurkov, Possible Operation of the European XFEL with Ultra-Low Emittance Beams, *Nucl. Instrum. and Methods* **A616**(2010)81–87.

- [18] E.L. Saldin, E.A. Schneidmiller and M.V. Yurkov, Nucl. Instrum. and Methods **A475**(2001)86.
- [19] G.T. Moore, Nucl. Instrum. and Methods **A239**(1985)19.
- [20] K.-J. Kim, Phys. Rev. Lett. **57**(1986)1871.
- [21] S. Krinsky and L. H. Yu, Phys. Rev. A **35**(1987)3406.
- [22] L.H. Yu, S. Krinsky and R.L. Gluckstern, Phys. Rev. Lett. **64**(1990)3011.
- [23] M. Xie, Nucl. Instrum. and Methods **A445**(2000)67.
- [24] E.L. Saldin, E. A. Schneidmiller, and M.V. Yurkov, Opt. Commun. 235(2004)415.
- [25] E.L. Saldin, E.A. Schneidmiller, and M.V. Yurkov, Opt. Commun. **186**(2000)185.